Non-Fermi-Liquid Behavior from Cavity Electromagnetic Vacuum Fluctuations at the Superradiant Transition

Peng Rao and Francesco Piazza
Max Planck Institute for the Physics of Complex Systems, Nöthnitzer Straße 38, 01187 Dresden, Germany

(Received 25 July 2022; revised 9 December 2022; accepted 6 February 2023; published 23 February 2023)

We study two-dimensional materials where electrons are coupled to the vacuum electromagnetic field of a cavity. We show that, at the onset of the superradiant phase transition towards a macroscopic photon occupation of the cavity, the critical electromagnetic fluctuations, consisting of photons strongly overdamped by their interaction with electrons, can in turn lead to the absence of electronic quasiparticles. Since transverse photons couple to the electronic current, the appearance of non-Fermi-Liquid behavior strongly depends on the lattice. In particular, we find that in a square lattice the phase space for electron-photon scattering is reduced in such a way to preserve the quasiparticles, while in a honeycomb lattice the latter are removed due to a nonanalytical frequency dependence of the damping $\propto |\omega|^{2/3}$. Standard cavity probes could allow us to measure the characteristic frequency spectrum of the overdamped critical electromagnetic modes responsible for the non-Fermi-liquid behavior.

DOI: 10.1103/PhysRevLett.130.083603

Introduction.—Certain strongly correlated metals do not behave according to Landau's Fermi-liquid theory (see Ref. [1] for a recent classification). In most of the cases this happens in correspondence to a quantum critical point separating a normal metallic phase and a symmetry-broken phase [2,3]. Within this scenario which has special relevance in two-dimensional materials, the strong coupling between the Fermi surface and critical order-parameter fluctuations leads to the loss of Landau's quasiparticles and thus to non-Fermi-Liquid behavior [4–19]. A direct signature is a nonanalytical frequency dependence of the quasiparticle damping $\sim|\omega|^{\alpha}$, with $\alpha < 1$, as opposed to the usual Fermi-liquid damping $\sim\omega^2$ which becomes instead increasingly irrelevant towards the Fermi surface $\omega \to 0$. In order to improve our understanding of the emergence of non-Fermi-liquid behavior and its experimental relevance, it would be highly desirable to determine the microscopic origin of the bosonic degree of freedom whose critical fluctuations are responsible for removing the electronic quasiparticles.

The recent experimental possibility to strongly couple electrons in two-dimensional materials with photons confined within cavities [20,21] has opened new avenues for controlling collective electronic phenomena and explore them in novel scenarios. These include cavity induced superconductivity [22–30], magnetism [31–35], ferroelectricity [36,37], as well as topological phenomena [38–45], that could be realized by engineering the quantum electrodynamical (QED) coupling between matter and light. These scenarios can also be investigated with synthetic matter made of ultracold atoms [46].

In this Letter, we show that cavity QED within two-dimensional materials offers ideal conditions to implement and observe non-Fermi-liquid behavior. The fluctuations of the emergent bosonic degree of freedom which induce non-Fermi-liquid behavior in the standard scenario are here substituted by the fluctuations of the vacuum electromagnetic field, i.e., a microscopic degree of freedom whose dynamics and coupling with electrons can be controlled by cavity engineering. Moreover, two-dimensional materials within layered structures [21] (and even more so synthetic ultracold-atomic systems [46–48]) offer an enhanced tunability of electronic properties, including Coulomb interactions as well as the role of impurities and phonons. This potentially allows us to realize a situation where the QED coupling with cavity photons is dominant. Cavity mirrors create a gap in the electromagnetic spectrum. However, electromagnetic modes can be made critical by reaching the transition point towards superradiance [49–56], at which the hybridization with the matter creates gapless polariton modes. Since the QED coupling depends on the electron momentum, we find that non-Fermi-liquid behavior can be controlled via the choice of the underlying lattice. We consider here a square and a honeycomb lattice away from unit filling. While in both cases the hybridization with matter leads to overdamped polaritons at the critical point, the phase space for electron-photon scattering is such that

non-Fermi-liquid behavior is absent for the square lattice, where the electron quasiparticle damping is $\propto \omega^2 \log|\omega|$, but present for the honeycomb lattice, where the damping is $\propto |\omega|^{2/3}$. Measurements of the cavity spectrum could show, instead of a well-defined resonance, nonanalytical power-law tails revealing the presence of the critical bosonic fluctuations responsible for the non-Fermi-liquid behavior. The present scenario can also be realized with ultracold fermionic atoms in confocal cavities [57].

Model.—We consider the cavity consisting of two parallel perfect conducting mirrors and choose the Coulomb gauge: $\mathrm{div}\,\mathbf{A} = 0$ for the electromagnetic field. The two-dimensional electronic system is placed in the middle of the two plates as illustrated in Fig. 1. Because of the boundary condition at the mirrors, the nth photon modes acquire a finite "mass" $\omega_{0n} = n\pi/L$ where L is the distance between two plates [58]. For simplicity we shall consider only the $n = 1$ modes. Since, as we shall see, the relevant photon momenta for non-Fermi-liquid scaling are of the order of the inverse lattice constant $1/a$, this approximation is justified only for ultracold gases; for solid state systems $1/a$ instead exceeds the photon mass scale. However, as shown in the Supplemental Material [59], the inclusion of all cavity modes does not change the non-Fermi-liquid scaling. The photon dispersion is

$$\omega_k^2 = k^2 + \omega_0^2, \tag{1}$$

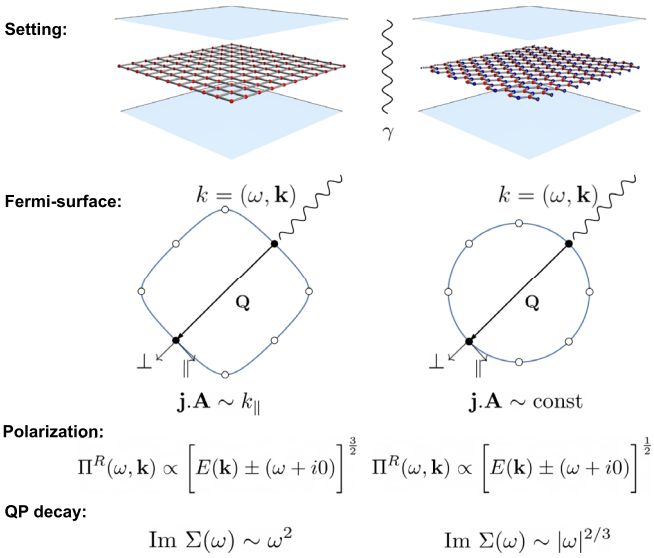

FIG. 1. Summary of the main results for the two cases considered: cavity photons coupled to electrons on a two-dimensional square lattice (left column) and honeycomb lattice (right column, red and blue atoms belong to the A, B sublattices). Potential hot spots are shown in white circles. For each lattice we show explicitly nesting momenta $\mathbf{Q}$ for one pair of hot spots in black dots. Note that on the honeycomb lattice, the entire Fermi surface is "hot."

where $\mathbf{k}$ is the 2D photon momentum in the plane of the lattice. The free particle Hamiltonian is

$$H_0 = -t \sum_{i,j,\alpha=\pm1} c^\dagger_{\alpha,i} c_{\alpha,j} + \sum_k \omega_k \left(b^\dagger_k b_k + \frac{1}{2} \right). \tag{2}$$

Here i, j are lattice sites and α is the spin index. The first term in (2) is the tight-binding electron Hamiltonian, and the second term describes the transverse photon modes. The free transverse photon Green's function has the form [58,59]

$$D_{0,ij}(\omega,\mathbf{k}) = -\frac{2}{L}\frac{1}{\omega^2 - \omega_k^2} e_i(\mathbf{k}) e_j^*(\mathbf{k}), \tag{3}$$

where $\mathbf{e}(\mathbf{k})$ is the transverse polarization vector: $\mathbf{k}.\mathbf{e}(\mathbf{k}) = 0$. Electron-photon coupling is introduced via the Peierls substitution: $c_i \to c_i \exp \int_{\mathbf{r}_0}^{\mathbf{r}_i} \mathbf{A}.d\mathbf{r}$ in H_0 [61]. For our purpose it is sufficient to keep the paramagnetic part linear in $\mathbf{A}$ [55]:

$$V = -\sum_{\mathbf{k}} \mathbf{j}(\mathbf{k}).\mathbf{A}(\mathbf{k}), \qquad H = H_0 + V. \tag{4}$$

In principle, higher-order terms are required for guaranteeing gauge invariance of the theory, but those do not influence the results in this Letter (see below). At $\omega = 0$, the longitudinal cavity mode decouples from electrons as a result of charge conservation $\mathbf{k}.\mathbf{j} = 0$. Therefore, at small frequency, only the transverse cavity mode couples strongly to the Fermi-surface, whereas the longitudinal mode is suppressed by ω^2. In what follows we shall only consider coupling between the transverse mode and electrons.

Superradiant critical point.—The light-matter coupling (4) leads to hybridization between cavity photons and electronic excitations. The properties of the resulting polariton modes are described by the Dyson's equation for the retarded transverse photon Green's function [see Fig. 2(b)]:

$$[D^R(k)]^{-1} = [D_0^R(k)]^{-1} - \Pi^R(k), \tag{5}$$

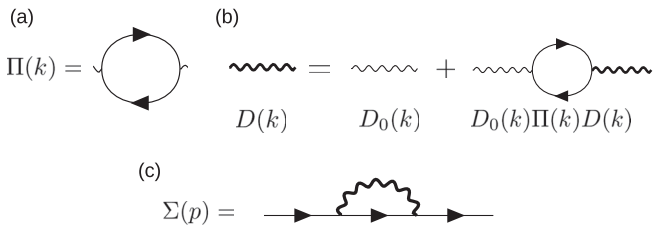

FIG. 2. One loop diagrammatic representation for (a) the polarization function $\Pi(k)$; (b) the Dyson equation for photon propagator $D(k)$; and (c) electron self-energy $\Sigma(p)$ renormalized by the thick photon (polariton) line in (b).

with the polarization function $\Pi^R(k)$. The superradiant critical point is reached at given momenta $\mathbf{k}$ such that the polariton gap closes: $\Pi^R(0,\mathbf{k}) = [D_0^R(0,\mathbf{k})]^{-1}$. Beyond this point a macroscopic occupation of photons at momenta $\mathbf{k}$ becomes energetically favorable. For the case of multiple cavity modes, $D^R(k)$ becomes a matrix in cavity mode indices. The critical point is reached when one of the eigenvalues of $[D^R(0,\mathbf{k})]^{-1}$ first becomes zero [56,59]. Note that superradiance cannot happen at vanishing photon momenta which corresponds to a pure gauge. In this case the paramagnetic contribution is cancelled exactly by the diamagnetic part [55,56]. In this Letter, we consider electrons on square and honeycomb lattices away from unit filling, when the Fermi surfaces have imperfect nesting. As we shall see next, superradiance is first reached at momenta $\mathbf{k} = \mathbf{Q}$, where $\mathbf{Q}$ is a nesting momentum. We will show that at the critical point the polariton modes are strongly overdamped at small frequencies and near momenta $\mathbf{Q}$, and these can in turn destroy the electronic quasiparticles.

Square lattice.—Let us start with the square lattice below unit filling. The current operator in the tight-binding approximation is given by

$$\mathbf{j}(\mathbf{k}) = \sum_{\mathbf{p}} \mathbf{\Lambda}(\mathbf{p},\mathbf{k}) c^\dagger_{\mathbf{p}+\mathbf{k}} c_{\mathbf{p}},$$
$$\mathbf{\Lambda}(\mathbf{p},\mathbf{k}) = -aet \sin\left[\left(\mathbf{p}+\frac{\mathbf{k}}{2}\right).\mathbf{a}_i\right]\frac{\mathbf{a}_i}{a}. \tag{6}$$

Here $\mathbf{a}_i$ is the ith lattice vector and a is the lattice constant. There are special points on the Fermi surface which couple most strongly to the transverse photons. Generally, such a hot-spot point has a symmetric partner on the opposite side of the Fermi surface. They are connected by a nesting momentum $\mathbf{Q}$ which there lies perpendicular to the Fermi surface. On the square lattice away from unit filling, they are four pairs indicated in Fig. 1. The nesting momentum $\mathbf{Q}$ is only shown for one such pair in the figure. At the hot spots the electron dispersion has the form (7)

$$\xi_\pm(\mathbf{k}) = \pm v_F k_\perp + \frac{k_\parallel^2}{2m}, \tag{7}$$

where $k_\perp$ and $k_\parallel$ are components of $\mathbf{k}$ parallel and orthogonal to $\mathbf{Q}$, and v_F, m are parameters of the Fermi surface. We have assumed that we are sufficiently away from unit filling that the Fermi velocity v_F, which vanishes at the corners of the square Fermi surface at unit filling, can be regarded as constant here. In all cases the current-photon vertex that connects pairs of hot spots in Eq. (6) has the same form:

$$\mathbf{\Lambda}.\mathbf{e} \approx -a^2 et\left(p_\parallel + \frac{k_\parallel}{2}\right). \tag{8}$$

Here $\mathbf{p}$ is the quasimomentum measured from one of the hot spots. The momentum-dependent vertex in (8) affects the one-loop polarization function for the transverse cavity photons. Given the superradiant critical point condition, $\Pi^R(0,\mathbf{Q}) = [D_0^R(0,\mathbf{Q})]^{-1}$ in (5), the expansion $\Pi^R(\omega,\mathbf{Q}+\mathbf{k}) - \Pi^R(0,\mathbf{Q})$ at small ω and $|\mathbf{k}|$ contains the following nonanalytical contribution from near the Fermi surface:

$$-\frac{a^4(et)^2 m^{\frac{3}{2}}}{6\pi v_F}([E(\mathbf{k})+\omega+i0]^{\frac{3}{2}} + [E(\mathbf{k})-\omega-i0]^{\frac{3}{2}}), \tag{9}$$

where $E(\mathbf{k}) = v_F k_\perp + k_\parallel^2/(4m)$. This term induces an imaginary part at large negative $E(\mathbf{k})$, corresponding to strong Landau damping of the polariton mode at the superradiant critical point:

$$[-|E(\mathbf{k})| \pm (\omega+i0)]^{\frac{3}{2}} \to \pm i[|E(\mathbf{k})| \mp (\omega+i0)]^{\frac{3}{2}}.$$

Subsequent terms in the expansion of $\Pi^R(k) - \Pi^R(0,\mathbf{Q})$ receive contributions far from the Fermi surface and can be written in powers of $E(\mathbf{k})$. They provide dynamics for the polaritons. The retarded photon Green's function thus becomes

$$D^R(\omega,\mathbf{Q}+\mathbf{k}) = ([E(\mathbf{k})+\omega+i0]^{\frac{3}{2}} + [E(\mathbf{k})-\omega-i0]^{\frac{3}{2}} + bE(\mathbf{k}) + c[E(\mathbf{k})]^2)^{-1}, \tag{10}$$

where we have included up to quadratic powers of $E(\mathbf{k})$ in the expansion [15]. The constants b and c are given by contributions far from the Fermi surface. Note that the free photon dispersion (1) gives in principle also powers of $\xi_+(\mathbf{k})$ in the denominator of D^R. These have been, however, neglected since they do not affect the quasiparticle decay, as will be justified below.

We now calculate the electronic quasiparticle decay as a function of frequency, due to the interaction with the Landau-damped polariton mode. The decay rate is given by twice the imaginary part of the electron self-energy, shown in Fig. 2(c):

$$\mathrm{Im}\Sigma^R\left(\omega,\frac{\mathbf{Q}}{2}\right) \propto \int k_\parallel^2 \mathrm{Im} D^R[\xi_+(\mathbf{k})-\omega, \mathbf{k}-\mathbf{Q}]\frac{d^2k}{(2\pi)^2}. \tag{11}$$

Here, $0 < \xi_+(\mathbf{k}) < \omega$. In Eq. (11), the photon Green's function at small frequency and near momenta $\mathbf{Q}$ is considered, which corresponds to the polariton mode. We evaluate this integral in the Supplemental Material [59]. Here we limit ourselves to highlighting the most important feature, namely, that at sufficiently small ω, the dominant contribution to (11) comes from the region in the

phase space in which polariton Landau damping is strong: $-E(\mathbf{k}) \gg \xi_+(\mathbf{k}) \sim \omega > 0$. This justifies neglecting $\xi_+(\mathbf{k})$. The final result is

$$\mathrm{Im}\Sigma^R\left(\omega, \frac{\mathbf{Q}}{2}\right) \sim \omega^2 \log|\omega|. \tag{12}$$

The electron quasiparticles remain thus well defined in this case. This can be attributed to the momentum dependence of the QED coupling (4) inherited from the electronic current operator (6), which suppresses the effect of the Landau-damped polaritons near the Fermi surface [compare with Eq. (17) on the honeycomb lattice below].

Honeycomb lattice.—We now turn to the honeycomb lattice. For simplicity we shall focus on the K' point in quasimomentum space. The single-particle Hamiltonian H_0 then has the form

$$H_0(\mathbf{k}) = v_F \boldsymbol{\sigma}.\mathbf{k}. \tag{13}$$

Here $\boldsymbol{\sigma}$ are Pauli matrices in pseudospin space and $\mathbf{k}$ is a 2D quasimomentum measured from K'. Equation (13) gives two particle-hole symmetric bands with energies $\varepsilon_\lambda(k)$ and eigenstates $u_\lambda(\mathbf{k})$:

$$\varepsilon_\lambda(k) = \lambda v_F k, \qquad u_\lambda(\mathbf{k}) = \frac{1}{\sqrt{2}}\begin{pmatrix} 1 \\ \lambda \exp(i\varphi_{\mathbf{k}}) \end{pmatrix}, \tag{14}$$

where $\lambda = \pm$ and $\varphi_{\mathbf{k}}$ is the polar angle of $\mathbf{k}$. At finite positive chemical potential μ, the Fermi surface is a circle on the electron band. Contrary to the square lattice case, the current operator has no momentum dependence:

$$\mathbf{j} = \frac{\delta}{\delta \mathbf{A}} H_0(\mathbf{k} - e\mathbf{A}) = -e v_F \boldsymbol{\sigma}. \tag{15}$$

Moreover, the whole Fermi surface is nested, i.e., $\mathbf{Q} = 2\mathbf{p}_F$. At low-enough energies, we will assume each of the infinitely many hot-spot pairs to contribute independently [12] and therefore consider only one such pair, with dispersion given by Eq. (7) with $m = p_F/v_F$. It gives a nonanalytical contribution to the polarization function quantified by the expansion around the critical point $\Pi^R(\omega, \mathbf{Q} + \mathbf{k}) - \Pi^R(0, \mathbf{Q})$, which reads

$$\frac{e^2 v_F \sqrt{m}}{2\pi}([E(\mathbf{k}) + \omega + i0]^{\frac{1}{2}} + [E(\mathbf{k}) - \omega - i0]^{\frac{1}{2}}), \tag{16}$$

where we have neglected terms of order k^2/p_F^2. The details of computing (16) are given in the Supplemental Materials [59]. In what follows, we include in (16) also a linear term in $E(\mathbf{k})$ for polartion dynamics. As is the case for the square lattice, powers of ξ_+ do not need to be included. Therefore, for large negative $E(\mathbf{k})$, we find strongly Landau damped polaritons at the superradiant critical point, albeit with a different nonanalytic power law.

The quasiparticle decay rate at the hot spots due to interactions with overdamped polaritons at small ω now becomes [59]

$$\mathrm{Im}\Sigma^R(\omega, \mathbf{p}_F) \sim |\omega|^{2/3}, \tag{17}$$

Therefore, the quasiparticle decay exhibits non-FL scaling contrary to the square lattice case, despite the presence of strong Landau damping for both lattices. This is because, on the honeycomb lattice, the dominant contribution comes from the region $-E(\mathbf{k}) \sim \Lambda_0(\omega/\Lambda_0)^{2/3} \gg \omega$, Λ_0 being a UV cutoff, whereas on the square lattice this region is suppressed by the additional powers of momenta from the current operator (6).

We note that the nonanalytical form of the quasiparticle damping in (17) is the same as predicted for noncommensurate charge-density-wave [4,15] and Fulde-Ferrel-Larkin-Ovchinnikov [16,17] quantum critical points. The same damping form is found for 2D fermionic systems with emergent $U(1)$ gauge fields as well, despite the important physical difference consisting in the gauge propagator being Landau damped at small frequencies and momenta [4,9,62]. We conclude this part by mentioning that the result (17) does not affect the polariton Landau damping (16), which is induced by electrons at large momenta. This is typically the case for one-loop Eliashberg-type theories [63].

Implementation.—The light-matter coupling (4) is relevant for electrons in solid state, which couple to photons via the current [21]. For neutral atomic gases instead, the dispersive coupling between photons and the atomic center of mass is independent of the momentum of the latter [46]. Therefore, non-Fermi-liquid behavior of Eq. (17) will be present regardless of the lattice, as long as unit filling is avoided. The same situation can be engineered also in solid state using two-photon transitions exploiting the diamagnetic coupling [64] or auxiliary electronic bands [34].

Accessibility.—The accessibility of our non-Fermi-liquid regime relies upon reaching the superradiant transition. In the solid-state microcavity setup, the related challenges have been addressed in Refs. [55,56]. Here one must also consider higher cavity modes $n \neq 1$, but the non-FL scaling remains unaffected [59]. On the other hand, for ultracold Fermi gases superradiance has been already observed [65], albeit only with a single isolated cavity mode. The required extension to a 2D continuum of modes is available in confocal cavities [57,66].

Observability.—With the purpose of probing the non-Fermi-liquid behavior, layered structures allow us to precisely measure the electronic spectral function of an embedded 2D material using techniques like momentum-and-energy-resolved tunneling spectroscopy (MERTS) [67] and thus potentially to directly probe the nonanalytic

behavior of the quasiparticle damping. Such measurements are standardly available also for neutral atomic gases through radio-frequency spectroscopy [68].

Since in our scenario the bosonic order parameter fluctuations affecting the electrons are in fact photons, cavity probes can provide direct access to their characteristic overdamped behavior responsible in turn for the electronic quasiparticle damping. At sufficiently low frequencies $|\omega| < -E(\mathbf{k})$, the usual resonant peaks in the cavity spectral function $A(\omega, \mathbf{Q}+\mathbf{k}) = \mathrm{Im}D^R(\omega, \mathbf{Q}+\mathbf{k})/\pi$ are substituted by a continuum of overdamped modes:

$$A(\omega, \mathbf{Q}+\mathbf{k}) \sim \frac{[\omega + |E(\mathbf{k})|]^\alpha - [|E(\mathbf{k})| - \omega]^\alpha}{\{[\omega + |E(\mathbf{k})|]^\alpha - [|E(\mathbf{k})| - \omega]^\alpha\}^2 + b^2 E(\mathbf{k})^2}, \tag{18}$$

where $\alpha = 3/2$ for the square lattice and $\alpha = 1/2$ for the honeycomb. The distinct power-law dependence in (18) at small ω can be an experimental signature of the critical electromagnetic fluctuations affecting the electrons. While such frequency- and momentum-resolved cavity probes are available in state-of-the-art experiments with atomic gases at the relevant frequencies and momenta [69], they seem rather challenging in the solid-state case, since the momentum scale $Q \sim p_F$ is much larger than the characteristic photon wave vectors.

Conclusions.—We have shown that cavity QED with 2D materials allows us to implement and probe non-Fermi-liquid behavior under pristine conditions: (i) the underlying critical bosonic fluctuations which destroy the electronic quasiparticles are provided by the electromagnetic vacuum field and are thus controllable via cavity engineering; (ii) 2D materials (or the synthetic versions based on ultracold gases) allow for enhanced tunability of electronic properties and control over unwanted effects.

Our Letter introduces a new (experimentally relevant) model for the emergence of non-Fermi-liquid behavior, thus offering a new playground for controlled experimental investigations as well as for theoretical approaches.

Future studies shall provide improved theories for the superradiant criticality and the associated non-Fermi-liquid behavior (also including the unit-filling case on the square lattice where logarithmic divergences appear in the polarization), possibly identifying deviations from the universality class predicted for noncommensurate charge-density wave [4,15] or Fulde-Ferrel-Larkin-Ovchinnikov [16,17] quantum critical points.

We thank Ahana Chakraborty and Bernhard Frank for discussions.

[1] D. Chowdhury, Y. Werman, E. Berg, and T. Senthil, Translationally Invariant Non-Fermi-Liquid Metals with Critical Fermi Surfaces: Solvable Models, Phys. Rev. X **8**, 031024 (2018).

[2] H. v. Löhneysen, A. Rosch, M. Vojta, and P. Wölfle, Fermi-liquid instabilities at magnetic quantum phase transitions, Rev. Mod. Phys. **79**, 1015 (2007).

[3] G. R. Stewart, Non-Fermi-liquid behavior in d- and f-electron metals, Rev. Mod. Phys. **73**, 797 (2001).

[4] B. L. Altshuler, L. B. Ioffe, and A. J. Millis, Low-energy properties of fermions with singular interactions, Phys. Rev. B **50**, 14048 (1994).

[5] Y. B. Kim, A. Furusaki, X.-G. Wen, and P. A. Lee, Gauge-invariant response functions of fermions coupled to a gauge field, Phys. Rev. B **50**, 17917 (1994).

[6] A. Abanov, A. V. Chubukov, and J. Schmalian, Quantum-critical theory of the spin-fermion model and its application to cuprates: Normal state analysis, Adv. Phys. **52**, 119 (2003).

[7] A. V. Chubukov and D. L. Maslov, Nonanalytic corrections to the Fermi-liquid behavior, Phys. Rev. B **68**, 155113 (2003).

[8] W. Metzner, D. Rohe, and S. Andergassen, Soft Fermi Surfaces and Breakdown of Fermi-Liquid Behavior, Phys. Rev. Lett. **91**, 066402 (2003).

[9] S.-S. Lee, Low-energy effective theory of Fermi surface coupled with U(1) gauge field in $2+1$ dimensions, Phys. Rev. B **80**, 165102 (2009).

[10] D. Dalidovich and S.-S. Lee, Perturbative non-Fermi liquids from dimensional regularization, Phys. Rev. B **88**, 245106 (2013).

[11] I. Mandal and S.-S. Lee, Ultraviolet/infrared mixing in non-Fermi liquids, Phys. Rev. B **92**, 035141 (2015).

[12] M. A. Metlitski and S. Sachdev, Quantum phase transitions of metals in two spatial dimensions. I. Ising-nematic order, Phys. Rev. B **82**, 075127 (2010).

[13] M. A. Metlitski and S. Sachdev, Quantum phase transitions of metals in two spatial dimensions. II. Spin density wave order, Phys. Rev. B **82**, 075128 (2010).

[14] K. V. Samokhin and M. S. Mar'enko, Quantum fluctuations in Larkin-Ovchinnikov-Fulde-Ferrell superconductors, Phys. Rev. B **73**, 144502 (2006).

[15] T. Holder and W. Metzner, Non-Fermi-liquid behavior at the onset of incommensurate $2k_F$ charge- or spin-density wave order in two dimensions, Phys. Rev. B **90**, 161106(R) (2014).

[16] F. Piazza, W. Zwerger, and P. Strack, FFLO strange metal and quantum criticality in two dimensions: Theory and application to organic superconductors, Phys. Rev. B **93**, 085112 (2016).

[17] D. Pimenov, I. Mandal, F. Piazza, and M. Punk, Non-Fermi liquid at the FFLO quantum critical point, Phys. Rev. B **98**, 024510 (2018).

[18] S.-S. Lee, Recent developments in non-Fermi liquid theory, Annu. Rev. Condens. Matter Phys. **9**, 227 (2018).

[19] G. Driskell, S. Lederer, C. Bauer, S. Trebst, and E.-A. Kim, Identification of Non-Fermi Liquid Physics in a Quantum Critical Metal via Quantum Loop Topography, Phys. Rev. Lett. **127**, 046601 (2021).

[20] F. J. Garcia-Vidal, C. Ciuti, and T. W. Ebbesen, Manipulating matter by strong coupling to vacuum fields, Science **373**, eabd0336 (2021).

[21] F. Schlawin, D. M. Kennes, and M. A. Sentef, Cavity quantum materials, Appl. Phys. Rev. **9**, 011312 (2022).

[22] E. Colella, R. Citro, M. Barsanti, D. Rossini, and M.-L. Chiofalo, Quantum phases of spinful Fermi gases in optical cavities, Phys. Rev. B **97**, 134502 (2018).
[23] M. A. Sentef, M. Ruggenthaler, and A. Rubio, Cavity quantum-electrodynamical polaritonically enhanced electron-phonon coupling and its influence on superconductivity, Sci. Adv. **4**, eaau6969 (2018).
[24] F. Schlawin, A. Cavalleri, and D. Jaksch, Cavity-Mediated Electron-Photon Superconductivity, Phys. Rev. Lett. **122**, 133602 (2019).
[25] F. Schlawin and D. Jaksch, Cavity-Mediated Unconventional Pairing in Ultracold Fermionic Atoms, Phys. Rev. Lett. **123**, 133601 (2019).
[26] J. B. Curtis, Z. M. Raines, A. A. Allocca, M. Hafezi, and V. M. Galitski, Cavity Quantum Eliashberg Enhancement of Superconductivity, Phys. Rev. Lett. **122**, 167002 (2019).
[27] A. Thomas, E. Devaux, K. Nagarajan, T. Chervy, M. Seidel, D. Hagenmüller, S. Schütz, J. Schachenmayer, C. Genet, G. Pupillo, and T. W. Ebbesen, Exploring superconductivity under strong coupling with the vacuum electromagnetic field, arXiv:1911.01459.
[28] A. Sheikhan and C. Kollath, Cavity-induced superconducting and $4k_F$ charge-density-wave states, Phys. Rev. A **99**, 053611 (2019).
[29] J. Li and M. Eckstein, Manipulating Intertwined Orders in Solids with Quantum Light, Phys. Rev. Lett. **125**, 217402 (2020).
[30] A. Chakraborty and F. Piazza, Long-Range Photon Fluctuations Enhance Photon-Mediated Electron Pairing and SuperConductivity, Phys. Rev. Lett. **127**, 177002 (2021).
[31] F. Mivehvar, H. Ritsch, and F. Piazza, Cavity-Quantum-Electrodynamical Toolbox for Quantum Magnetism, Phys. Rev. Lett. **122**, 113603 (2019).
[32] M. Kiffner, J. R. Coulthard, F. Schlawin, A. Ardavan, and D. Jaksch, Manipulating quantum materials with quantum light, Phys. Rev. B **99**, 085116 (2019).
[33] M. A. Sentef, J. Li, F. Künzel, and M. Eckstein, Quantum to classical crossover of Floquet engineering in correlated quantum systems, Phys. Rev. Res. **2**, 033033 (2020).
[34] A. Chiocchetta, D. Kiese, C. P. Zelle, F. Piazza, and S. Diehl, Cavity-induced quantum spin liquids, Nat. Commun. **12**, 5901 (2021).
[35] J. B. Curtis, A. Grankin, N. R. Poniatowski, V. M. Galitski, P. Narang, and E. Demler, Cavity magnon-polaritons in cuprate parent compounds, Phys. Rev. Res. **4**, 013101 (2022).
[36] Y. Ashida, A. Imamoglu, J. Faist, D. Jaksch, A. Cavalleri, and E. Demler, Quantum Electrodynamic Control of Matter: Cavity-Enhanced Ferroelectric Phase Transition, Phys. Rev. X **10**, 041027 (2020).
[37] S. Latini, D. Shin, S. A. Sato, C. Schäfer, U. D. Giovannini, H. Hübener, and A. Rubio, The ferroelectric photo ground state of $SrTio_3$: Cavity materials engineering, Proc. Natl. Acad. Sci. U.S.A. **118**, e2105618118 (2021).
[38] J.-S. Pan, X.-J. Liu, W. Zhang, W. Yi, and G.-C. Guo, Topological Superradiant States in a Degenerate Fermi Gas, Phys. Rev. Lett. **115**, 045303 (2015).
[39] B. Gulácsi and B. Dóra, From Floquet to Dicke: Quantum Spin Hall Insulator Interacting with Quantum Light, Phys. Rev. Lett. **115**, 160402 (2015).
[40] W. Zheng and N. R. Cooper, Superradiance Induced Particle Flow via Dynamical Gauge Coupling, Phys. Rev. Lett. **117**, 175302 (2016).
[41] C. Kollath, A. Sheikhan, S. Wolff, and F. Brennecke, Ultracold Fermions in a Cavity-Induced Artificial Magnetic Field, Phys. Rev. Lett. **116**, 060401 (2016).
[42] F. Mivehvar, H. Ritsch, and F. Piazza, Superradiant Topological Peierls Insulator inside an Optical Cavity, Phys. Rev. Lett. **118**, 073602 (2017).
[43] X. Wang, E. Ronca, and M. A. Sentef, Cavity quantum electrodynamical chern insulator: Towards light-induced quantized anomalous Hall effect in graphene, Phys. Rev. B **99**, 235156 (2019).
[44] F. Appugliese, J. Enkner, G. L. Paravicini-Bagliani, M. Beck, C. Reichl, W. Wegscheider, G. Scalari, C. Ciuti, and J. Faist, Breakdown of topological protection by cavity vacuum fields in the integer quantum Hall effect, Science **375**, 1030 (2022).
[45] V. Rokaj, M. Penz, M. A. Sentef, M. Ruggenthaler, and A. Rubio, Polaritonic Hofstadter butterfly and cavity control of the quantized Hall conductance, Phys. Rev. B **105**, 205424 (2022).
[46] F. Mivehvar, F. Piazza, T. Donner, and H. Ritsch, Cavity QED with quantum gases: New paradigms in many-body physics, Adv. Phys. **70**, 1 (2021).
[47] K. Roux, H. Konishi, V. Helson, and J.-P. Brantut, Strongly correlated fermions strongly coupled to light, Nat. Commun. **11**, 2974 (2020).
[48] X. Zhang, Y. Chen, Z. Wu, J. Wang, J. Fan, S. Deng, and H. Wu, Observation of a superradiant quantum phase transition in an intracavity degenerate Fermi gas, Science **373**, 1359 (2021).
[49] F. Piazza and P. Strack, Umklapp Superradiance with a Collisionless Quantum Degenerate Fermi Gas, Phys. Rev. Lett. **112**, 143003 (2014).
[50] J. Keeling, M. J. Bhaseen, and B. D. Simons, Fermionic Superradiance in a Transversely Pumped Optical Cavity, Phys. Rev. Lett. **112**, 143002 (2014).
[51] Y. Chen, Z. Yu, and H. Zhai, Superradiance of Degenerate Fermi Gases in a Cavity, Phys. Rev. Lett. **112**, 143004 (2014).
[52] P. Nataf, T. Champel, G. Blatter, and D. M. Basko, Rashba Cavity QED: A Route Towards the Superradiant Quantum Phase Transition, Phys. Rev. Lett. **123**, 207402 (2019).
[53] G. M. Andolina, F. M. D. Pellegrino, V. Giovannetti, A. H. MacDonald, and M. Polini, Cavity quantum electrodynamics of strongly correlated electron systems: A no-go theorem for photon condensation, Phys. Rev. B **100**, 121109(R) (2019).
[54] M. Schuler, D. D. Bernardis, A. M. Läuchli, and P. Rabl, The vacua of dipolar cavity quantum electrodynamics, SciPost Phys. **9**, 66 (2020).
[55] D. Guerci, P. Simon, and C. Mora, Superradiant Phase Transition in Electronic Systems and Emergent Topological Phases, Phys. Rev. Lett. **125**, 257604 (2020).
[56] G. M. Andolina, F. M. D. Pellegrino, V. Giovannetti, A. H. MacDonald, and M. Polini, Theory of photon condensation

in a spatially varying electromagnetic field, Phys. Rev. B **102**, 125137 (2020).
[57] C. Rylands, Y. Guo, B. L. Lev, J. Keeling, and V. Galitski, Photon-Mediated Peierls Transition of a 1d Gas in a Multimode Optical Cavity, Phys. Rev. Lett. **125**, 010404 (2020).
[58] K. Kakazu and Y. S. Kim, Quantization of electromagnetic fields in cavities and spontaneous emission, Phys. Rev. A **50**, 1830 (1994).
[59] See Supplemental Material at http://link.aps.org/supplemental/10.1103/PhysRevLett.130.083603 for quantization of the cavity photon field and computational details, which also includes Ref. [60].
[60] L. Landau, J. Bell, M. Kearsley, L. Pitaevskii, E. Lifshitz, and J. Sykes, *Electrodynamics of Continuous Media*, Course of Theoretical Physics (Elsevier Science, New York, 2013).
[61] Under the Coulomb gauge, the scalar potential ϕ mediates direct Coulomb interactions between electrons. Since Coulomb interactions are not expected to generate non-FL behavior, we shall neglect ϕ in this Letter.
[62] I. Mandal, Critical Fermi surfaces in generic dimensions arising from transverse gauge field interactions, Phys. Rev. Res. **2**, 043277 (2020).
[63] J. Polchinski, Low-energy dynamics of the spinon-gauge system, Nucl. Phys. **B422**, 617 (1994).
[64] H. Gao, F. Schlawin, M. Buzzi, A. Cavalleri, and D. Jaksch, Photoinduced Electron Pairing in a Driven Cavity, Phys. Rev. Lett. **125**, 053602 (2020).
[65] X. Zhang, Y. Chen, Z. Wu, J. Wang, J. Fan, S. Deng, and H. Wu, Observation of a superradiant quantum phase transition in an intracavity degenerate Fermi gas, Science **373**, 1359 (2021).
[66] A. J. Kollár, A. T. Papageorge, K. Baumann, M. A. Armen, and B. L. Lev, An adjustable-length cavity and Bose–Einstein condensate apparatus for multimode cavity QED, New J. Phys. **17**, 043012 (2015).
[67] J. Jang, H. M. Yoo, L. Pfeiffer, K. West, K. Baldwin, and R. C. Ashoori, Full momentum-and energy-resolved spectral function of a 2d electronic system, Science **358**, 901 (2017).
[68] M. Punk and W. Zwerger, Theory of RF-Spectroscopy of Strongly Interacting Fermions, Phys. Rev. Lett. **99**, 170404 (2007).
[69] R. Mottl, F. Brennecke, K. Baumann, R. Landig, T. Donner, and T. Esslinger, Roton-type mode softening in a quantum gas with cavity-mediated long-range interactions, Science **336**, 1570 (2012).